CDF note 9413

Search for the Decays $\mathbf{B^0_{s,d} \to e^+\mu^-}$ and $\mathbf{B^0_{s,d} \to e^+e^-}$

The CDF Collaboration
URL http://www-cdf.fnal.gov

(Dated: July 17, 2008)

We report on a search for the lepton flavor violation Decays of $B^0_{s,d} \to e^+\mu^-$ and the flavor changing neutral current decays $B^0_{s,d} \to e^+e^-$ using a 2 fb^{-1} data sample of p$\bar{\text{p}}$ collisions at $\sqrt{s} =$ 1.96 TeV collected with the CDF II detector at the Fermilab. We find one event in the search window for $B^0_s \to e^+\mu^-$ with estimated 0.81 ± 0.63 background events, two events for $B^0_d \to e^+\mu^-$ with 0.94 ± 0.63 estimated background events, one event for $B^0_s \to e^+e^-$ with 2.7 ± 1.8 estimated background events and two events for $B^0_d \to e^+e^-$ with 2.7 ± 1.8 estimated background events. Using 6387.0 ± 214.4 events of $B^0_d \to K^+\pi^-$ as a relative normalization, we derive the uppers limits on the decay branching ratios $Br(B^0_s \to e^+\mu^-) < 2.0\ (2.6) \times 10^{-7}$, $Br(B^0_d \to e^+\mu^-) <$ $6.4\ (7.9) \times 10^{-8}$, $Br(B^0_s \to e^+e^-) < 2.8\ (3.7) \times 10^{-7}$ and $Br(B^0_d \to e^+e^-) < 8.3\ (10.6) \times 10^{-8}$ at 90 (95)% confidence level. From the decay branching ratio limits we calculate the corresponding lower bounds on the Pati-Salam leptoquark masses: $\mathrm{M_{LQ}}(B^0_s) > 47.7\ (44.6)$ TeV/c^2 for the B^0_s and $\mathrm{M_{LQ}}(B^0_d) > 58.6\ (55.7)$ TeV/c^2 for the B^0_d at 90 (95)% confidence level.

Preliminary Results for Summer 2008 Conferences

I. INTRODUCTION

The decays $B^0_{s,d} \to e^+\mu^-$ are forbidden within the Standard Model of particle physics in which leptons do not change flavor. These decays are allowed, however, in some extensions to the Standard Model, such as Pati-Salam model [1], some SUper SYmmetry (SUSY) model [2] or Extra Dimension (ED) models. In these models, the assumption of a local gauge symmetry between quarks and leptons at the lepton-flavor violation tree-level couplings leads to the prediction of a new force of nature which mediates transitions between quarks and leptons [3][4].

The Grand Unification Theory (GUT) by J. Pati and A. Salam predicts spin 1 gauge bosons the so called "Pati Salam Leptoquarks" (LQ) that carry both color and lepton quantum numbers [1]. The lepton and quark components are not necessarily from the same generation [3][4] and can mediate the decays of $B^0_s \to e^+\mu^-$ and $B^0_d \to e^+\mu^-$ as shown in Figure 1, with different types of leptoquarks [3][4].

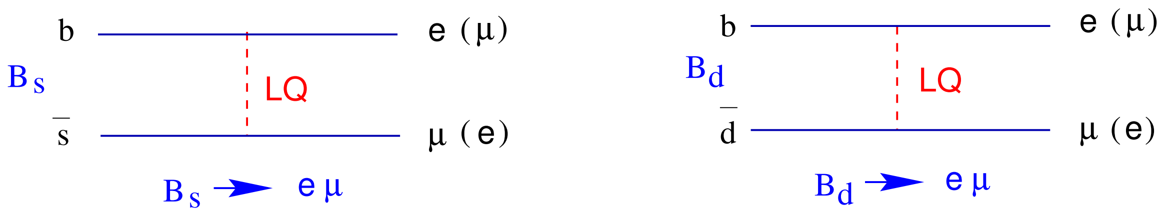

FIG. 1: Feynman diagrams for the lepton flavor violation decays $B^0_s \to e^+\mu^-$ and $B^0_d \to e^+\mu^-$ decays mediated by Pati-Salam leptoquarks (LQ).

The Flavor Changing Neutral Current (FCNC) decays of $B^0_{s,d} \to e^+e^-$, shown in Figure 2, are further suppressed comparing to $B^0_{s,d} \to \mu^+\mu^-$ by the ratio of electron and muon masses $(m_e/m_\mu)^2$. The Standard Model predicts these FCNC $B^0_{s,d}$ decays into di-electrons with a decay branching ratio in the order of 10^{-15} [5] which is much smaller than the 10^{-9} for $B^0_{s,d} \to \mu^+\mu^-$. So while $B^0_{s,d} \to \mu^+\mu^-$ starts to put serious constrains on various models, there is plenty of wiggle room left in the case for $B^0_{s,d} \to e^+e^-$. The current experimental sensitivities from CDF and the B-factories on the decay branching ratio measurements of these decays are still below 10^{-8}. Any evidence of such signal showing up in the current data would indicate new physics beyond the Standard Model.

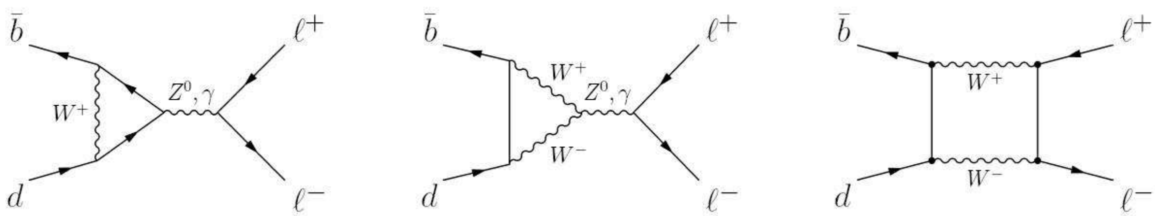

FIG. 2: Feynman diagrams for the flavor changing neutral current decays $B^0_d \to \ell^+\ell^-$ in the Standard Models.

In this paper, we report a search for these rare B decays using a data sample collected with the CDF II detector at $\sqrt{s} = 1.96$ TeV at the Fermilab Tevatron $p\bar{p}$-collider between August 2002 and March 2007 corresponding to an integrated luminosity of 2 fb^{-1}.

II. EVENT RECONSTRUCTION

The CDF II detector is described in detail elsewhere [6]. Here we describe the components of the detector most relevant for this analysis. The tracking system consists of a Silicon strip VerteX detector (SVX II) [7] and a drift chamber operating in a magnetic field of 1.4 T provided by a super-conducting solenoid. The SVX II system consists of 5 concentric silicon layers made of double-sided silicon. One side contains strips oriented axially along the beam direction, on the other side strips are rotated by a stereo angle. Layers 0, 1 and 3 use a 90^o stereo angle, while layers 2 and 4 utilize shallow-angle stereo at 1.2^o. The silicon system extends in radius from 2.5 cm to 10.6 cm. The impact parameter resolution for tracks with a transverse momentum p_T greater than 2 GeV/c is 40 μm, this is mainly due to a 30 μm contribution from the beam-spot. The Central Outer Tracker (COT) [8] is a drift chamber with an open-cell design and is segmented radially into eight super-layers. Each super-layer contains a plane of 12 sense wires tilted by 35^o with respect to the radial direction to compensate for the drift Lorentz angle. Super-layers alternate between axial and $\pm 2^o$ stereo orientation. The total drift chamber is 310 cm long with inner and outer radii of 41 cm and 138 cm respectively providing a long lever arm for curvature measurements. The achieved momentum resolution is $\sigma(p_T)/p_T^2 = 0.0015(\text{GeV}/c)^{-1}$. Outside the COT are electromagnetic [9] and hadronic calorimeters [10] arranged in a projective-tower geometry, covering the pseudo-rapidity region $|\eta| < 3.5$. Muon detectors consisting of multi-layer drift chambers are located radially around the outside of the calorimeter [6]. The Central Muon Unit (CMU) [11] covers a range in pseudo-rapidity of $|\eta| < 0.6$, where $\eta = -\ln(\tan\frac{\theta}{2})$ and θ is the polar angle. The Central Muon eXtension (CMX) extends the pseudo-rapidity range to $0.6 < |\eta| < 1.0$.

The event reconstruction for all decay channels in this paper starts from a data sample enriched with two-body B decays selected with set of requirements implemented in the eXtremely Fast Tracker (XFT) [12] at Level-1 and the Silicon Vertex Trigger [13] at Level-2 of a three-level trigger system [14]. The selection [15] starts with the two opposite-charged tracks each with a transverse momentum $p_{T(1,2)} > 2\ GeV/c$ and an impact parameter with respect to the beam point$140\mu m d_0(1,2) < 1mm$. It also requires the track pair have the $p_{T1} + p_{T2} > 5.5GeV/c^2$, a transverse open-angle $20^o < \Delta\phi < 135^o$ and a transverse decay length of $L_{xy} > 200\mu m$. In the offline analysis, two additional selection cuts are applied to further reduce backgrounds. The isolation Iso which is defined as the ratio between the two-track B p_T and the sum of other tracks around B, and the pointing angle $\Delta\phi$ which is the angle between the transverse momentum vector of the reconstructed B and the vector pointing from the primary vertex to the B decay vertex. We optimized the two selections together with the L_{xy} and found the optimal values of the cuts as $\Delta\phi < 0.11$, Iso > 0.675 and $L_{xy} > 375\,\mu m$. Figure II shows the invariant mass distribution of the two-body B decay events passing the selections above, where we found 6387.0 ± 214.4 events of $B_d^0 \to K^+\pi^-$.

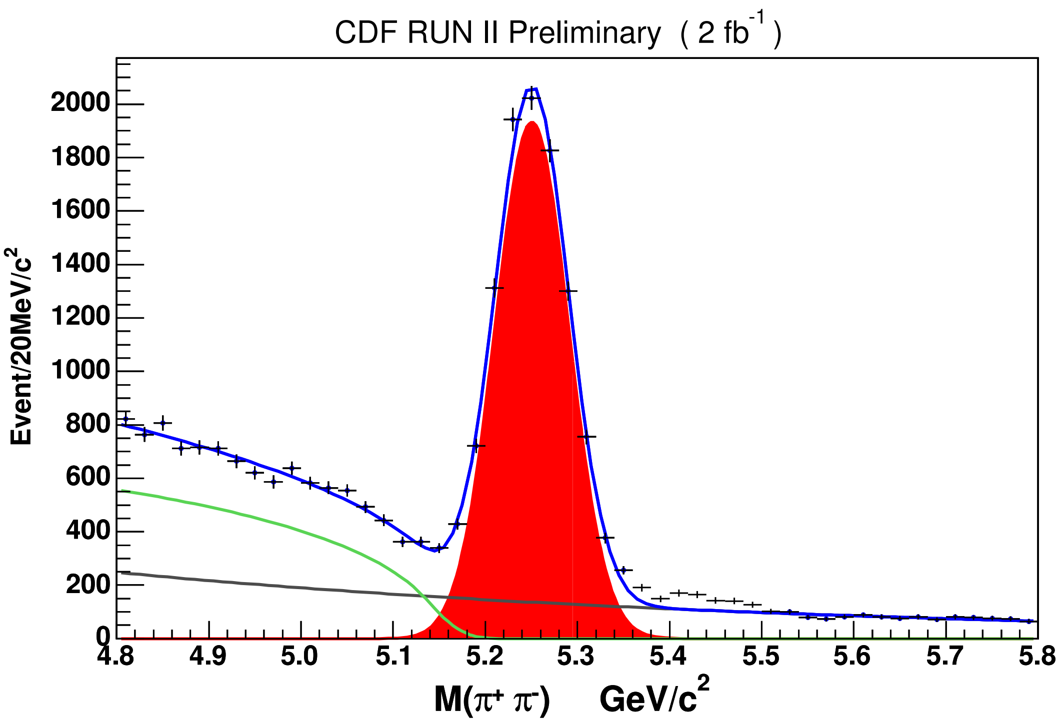

FIG. 3: Invariant mass distribution of the two-body B decays where each decay track assigned a pion mass. The result of a fit (blue line) is superimposed to the data (dots with error bars). The fitting function has three components: the two-body B decay signal (red filled area) parameterized as a Gaussian function, the combinatorial background (brown line) parameterized as an exponential, and the physics background (green line) parameterized as a smeared Argus function. Using the procedure described in reference [15], we estimate 6387.0 ± 214.4 events of $B_d^0 \to K^+\pi^-$ out of a total 9648.4 ± 224.7 two-body B decay.

Additional electron and muon identification are applied to the candidate of $B_{s,d}^0 \to e^+\mu^-$ and $B_{s,d}^0 \to e^+e^-$. Electron identification uses both specific ionization (dE/dx) information from the COT and calorimeter shower information from the Central ElectroMagnetic calorimeter. The logarithm of the ratio of the measured dE/dx value from a charged particle to that expected for an electron, $Z_e = \ln(dE/dx) - \ln(dE/dx)_{\text{predict}}$, is compared to its standard deviation

σ_{Z_e}. The expected dE/dx and σ_{Z_e} are functions of the particle charge, momentum, and the multiplicity of associated COT hits. Electron candidates are required to have $Z_e/\sigma_{Z_e} > -1.3$ to reject hadrons ($\pi/K/p$) while remaining efficient for true electrons. The dE/dx cut efficiencies as function of electron p_T are measured in pure samples of electrons from $\gamma \rightarrow e^+e^-$ to be around 90%. The calorimeter shower shape of a charged particle with p_T>2 GeV/c is obtained by extrapolating its track reconstructed in the COT into the calorimeter to match shower clusters there [16]. The calorimeter-based electron identification criteria using shower energy and shower cluster profiles are selected from comparing the distributions from pure electron and hadron. We found the efficiency for electrons is around 70% with this criteria for the p_T range interested in this paper. Muons are reconstructed from tracks measured in the tracking chambers matched to the stub positions in the CMU or CMX. The tracks are extrapolated to the CMU or CMX after using a simplified geometry model to track the muon candidate's motion in the non-uniform magnetic field of the calorimeter. The distance, $\Delta r\phi$, in the r-ϕ plane between the track projected to the muon chambers and the muon stub together with the measurement errors is used to select muons. The selection is close to be fully efficient for muons in CMU or CMX.

In Figure 4, we show the invariant mass distributions for $e^+\mu^-$ pairs and e^+e^- after all cuts including electron and muon identification have been applied. There is no signal found for these decays. We therefore use the information to set limits on the decay branching ratios.

III. LIMITS ON DECAY BRANCHING RATIOS

The signature of a signal from $B^0_{s,d}$ is a peak in the two-track invariant mass distribution which typically can be described by a Gaussian function. In the presence of energy loss due to electron Bremsstrahlung, the peak structure from $B^0_{s,d} \rightarrow e^+\mu^-$ and $B^0_{s,d} \rightarrow e^+e^-$ decays will be distorted by a long tail below the $B^0_{s,d}$ nominal mass, as shown in Figure 5 from a Monte Carlo simulation. Using nominal values for the $B^0_{s,d}$ masses from the Particle Data Book (PDG) [17] and the mass reconstruction resolution obtained from fitting the two-body B decays as in Figure II, the search windows are defined as (5.2616-5.4773) GeV/c^2 for $B^0_s \rightarrow e^+\mu^-$, (5.1713 - 5.3871) GeV/$c^2$ for $B^0_d \rightarrow e^+\mu^-$, (5.1542, 5.4773) GeV/$c^2$ for the $B^0_s \rightarrow e^+e^-$ and (5.064 - 5.3871) GeV/c^2 for the $B^0_d \rightarrow e^+e^-$.

For $B^0_{s,d} \rightarrow e^+\mu^-$, we observe one event in the B^0_s mass window and two events in the B^0_d mass window. These numbers are consistent with the number of events observed in the region outside the mass window. We estimate the background contributions to be 0.81 ± 0.63 events in the B^0_s mass window and 0.94 ± 0.63 in the B^0_d mass window from combinatorial and double lepton-fakes from two-body B decays. The combinatorial background is estimated to be 0.72 ± 0.63 for both B^0_s and B^0_d channels, from counting events outside the signal mass window, both low and high sideband in Figure 4, and normalizing this number to the size of the signal mass windows. The double e-μ fake events from two-body B decays is estimated as 0.09 ± 0.02 for B^0_s and 0.22 ± 0.04 for B^0_d, by counting events of two-body B decays in our search windows applying electron and muon fake rate to the two tracks found in Figure II.

For $B^0_{s,d} \rightarrow e^+e^-$, we observe one event in the B^0_s mass window and two events in the B^0_d mass window. The background contributions are estimated using similar method as for the $e^+\mu^-$ channels. We estimate the background contributions to be 2.7 ± 1.8 events in both the B^0_s or B^0_d mass windows from combinatorial ($2.66 \pm 1.19 \pm 1.35$) and double electron-electron fakes (0.038 ± 0.008 for both B^0_s or B^0_d).

We use the reference channel of $B^0_d \rightarrow K^+\pi^-$ to set limit on the decay branching ratios. The decay branching ratio for $B^0_s \rightarrow e^+\mu^-$ and $B^0_d \rightarrow e^+\mu^-$ are calculated using the following formula:

$$Br(B^0_s \rightarrow e^+\mu^-) = \frac{N^{90\%}(B^0_s \rightarrow e^+\mu^-) \cdot Br(B^0_d \rightarrow K^+\pi^-) \cdot f_{B^0_d}/f_{B^0_s}}{\epsilon^{rel}_{B^0_s \rightarrow e^+\mu^-} \cdot N(B^0_d \rightarrow K^+\pi^-)}. \quad (1)$$

$$Br(B^0_d \rightarrow e^+\mu^-) = \frac{N^{90\%}(B^0_d \rightarrow e^+\mu^-) \cdot Br(B^0_d \rightarrow K^+\pi^-)}{\epsilon^{rel}_{B^0_d \rightarrow e^+\mu^-} \cdot N(B^0_d \rightarrow K^+\pi^-)}, \quad (2)$$

where $N^{90\%}(B^0_d \rightarrow e^+\mu^-)$, $N^{90\%}(B^0_s \rightarrow e^+\mu^-)$ are the calculated number of events with 90% confidence level for $B^0_d \rightarrow e^+\mu^-$ and $B^0_s \rightarrow e^+\mu^-$; $N(B^0_d \rightarrow K^+\pi^-) = 6387.0 \pm 214.4$ is the numbers events from the reference channel $B^0_d \rightarrow K^+\pi^-$; $\epsilon^{rel}_{B^0_d \rightarrow e^+\mu^-}$ and $\epsilon^{rel}_{B^0_s \rightarrow e^+\mu^-}$ are the detector acceptance and event selection efficiencies for observing $B^0_d \rightarrow e^+\mu^-$ and $B^0_s \rightarrow e^+\mu^-$ decays relative to $B^0_d \rightarrow K^+\pi^-$; and $f_{B^0_d}/f_{B^0_s}$ [18] is the ratio of the b-quark fragmentation probabilities at the Tevatron. $(0.398 \pm 0.012)/(0.103 \pm 0.014) = 3.86 \pm 0.59$, where the (anti-)correlation between the uncertainties has been accounted for [18].

Monte Carlo events with full detector and trigger simulation are used to calculate the ϵ^{rel}. Electron and muon detector fiducial coverages, electron and muon identification efficiencies are measured from pure electron data sample

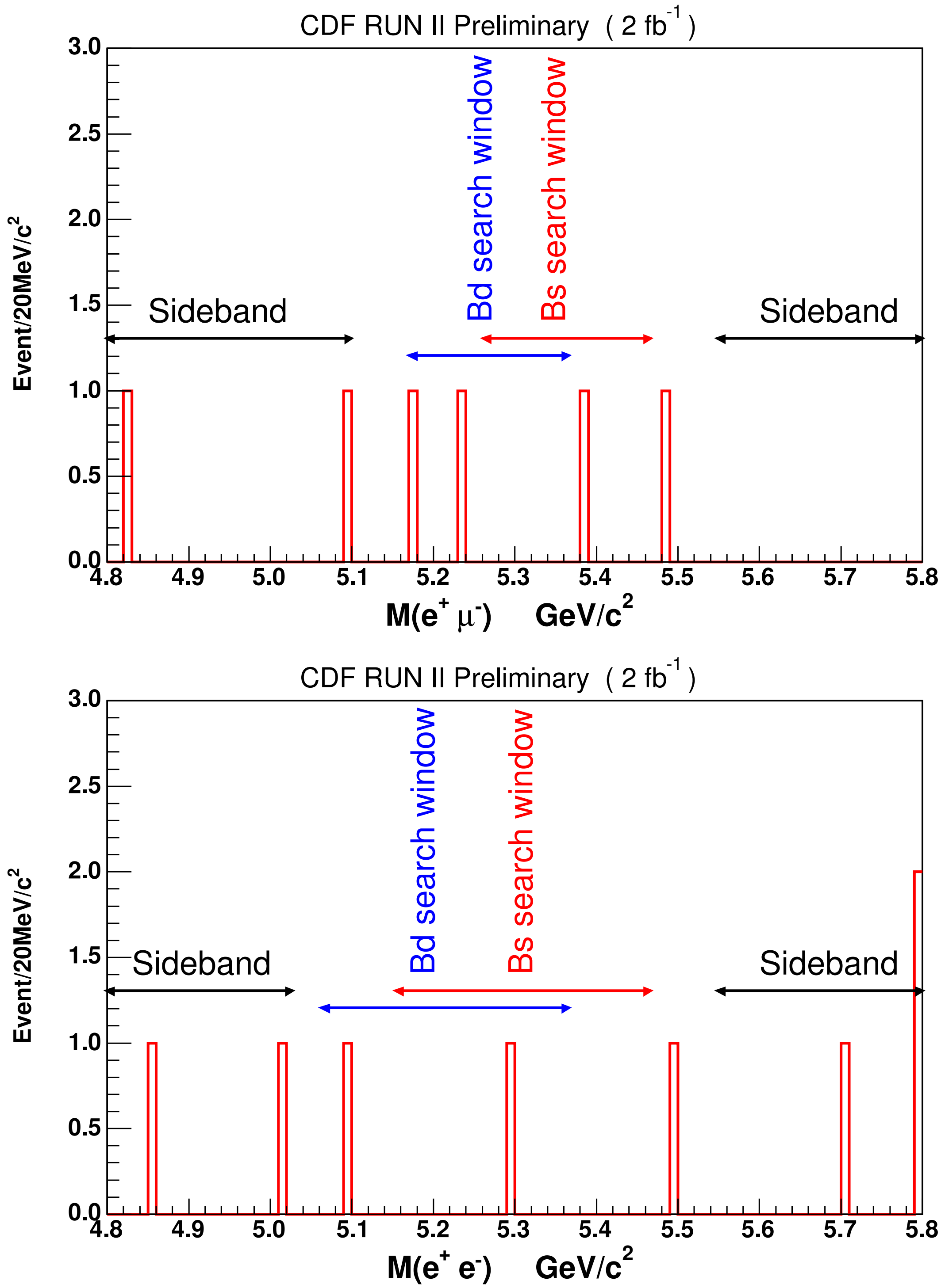

FIG. 4: Invariant mass distributions of the $e^+\mu^-$ (top) pairs and e^+e^- pairs (bottom) for events that passed both electron and muon identification. Mass windows indicated by red-colored arrows are for B_s^0 search window, blue-colored arrows for B_d^0 search window and black-colored arrows are for background estimation.

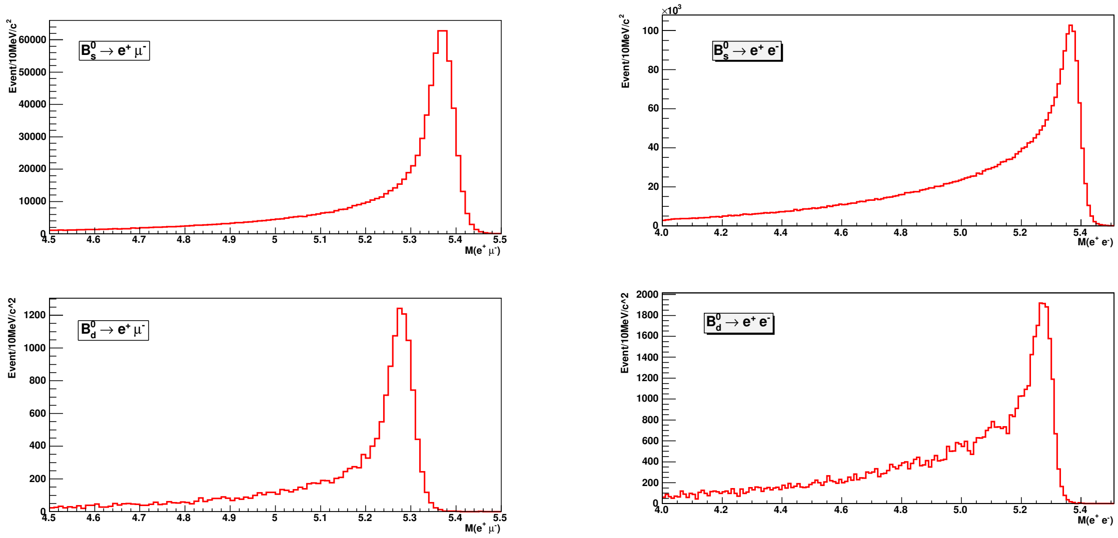

FIG. 5: Monte Carlo invariant mass distributions for $B^0_{s,d} \to e^+\mu^-$ (left plots) and $B^0_{s,d} \to e^+e^-$ (right plots)

and are convoluted in Monte Carlo events to take into considerations of kinematic correlations. We obtain $\epsilon^{rel}_{B^0_s \to e^+\mu^-} = 0.2071 \pm 0.0158$, $\epsilon^{rel}_{B^0_d \to e^+\mu^-} = 0.2097 \pm 0.0123$, $\epsilon^{rel}_{B^0_s \to e^+e^-} = 0.1290 \pm 0.011$ and $\epsilon^{rel}_{B^0_d \to e^+e^-} = 0.1278 \pm 0.011$. The errors listed above are the combined statistical and systematic errors which include uncertainties from detector fiducial coverages, electron and muon identification efficiencies, detector material accounting, $B^0_{s,d}$ p_T spectrum and $B^0_{s,d}$ lifetimes.

The upper limit of observed signal events in the search windows are obtained using the Bayesian approach [19] assuming a flat prior and incorporating Gaussian uncertainties into the limit. Total systematic errors, as listed in Table I and Table II, are used as input for the Bayesian limit calculation. We obtain the upper limit of observed signal events with 90% (95%) C.L. as: 3.60 (4.57) for $B^0_s \to e^+\mu^-$, 4.44 (5.44) for $B^0_d \to e^+\mu^-$, 3.11 (4.03) for $B^0_s \to e^+e^-$ and 3.51 (4.47) for $B^0_d \to e^+e^-$. The corresponding limits on the decay branching ratios are calculated as: $Br(B^0_s \to e^+\mu^-) < 2.0\ (2.6) \times 10^{-7}$, $Br(B^0_d \to e^+\mu^-) < 6.4\ (7.9) \times 10^{-8}$, $Br(B^0_s \to e^+e^-) < 2.8\ (3.7) \times 10^{-7}$ and $Br(B^0_d \to e^+e^-) < 8.3\ (10.6) \times 10^{-8}$ at 90 (95)% confidence level. These results represent a significant improvement compared to CDF's previous measurement and the best result from B-Factories. For the decay channel $B^0_s \to e^+e^-$, this is the first time such a limit has been obtained.

Source	values	ΔBr($B^0_s \to e^+\mu^-$)	ΔBr($B^0_d \to e^+\mu^-$)
$N(B^0 \to K^+\pi^-)$	6387.0 ± 214.4	3.4%	3.4%
$BR(B^0 \to K\pi)$	$(19.4 \pm 0.6) \times 10^{-6}$	3.1%	3.1%
$f_{B^0_d}/f_{B^0_s}$	3.86 ± 0.59	15.3%	-
$\epsilon^{Rel}_{B^0_s \to e^+\mu^-}$	0.2071 ± 0.0158	7.6%	-
$\epsilon^{Rel}_{B^0_d \to e^+\mu^-}$	0.2097 ± 0.0123	-	5.9%
Total		17.7%	7.5%

TABLE I: *Systematic uncertainties on the limits of $Br(B^0_{s,d} \to e^+\mu^-)$.*

IV. LIMITS ON THE LEPTOQUARK MASSES

Within the Pati-Salam leptoquark model [3], the following relationship between the Br($B^0_s \to e^+\mu^-$) and the leptoquark mass (M_{LQ}) can be derived:

$$Br(B^0_s \to e^+\mu^-) = \Gamma(B^0_s \to e^+\mu^-) \cdot \frac{\tau_{B^0_s}}{\hbar} = \pi\alpha_s(M_{LQ})\frac{1}{M^4_{LQ}}F^2_B m^3_B R^2 \cdot \frac{\tau_{B^0_s}}{\hbar} \qquad (3)$$

Source	values	$\Delta\mathrm{Br}(B_s^0 \to e^+e^-)$	$\Delta\mathrm{Br}(B_d^0 \to e^+e^-)$
$N(B^0 \to K^+\pi^-)$	6387.0 ± 214.4	3.4%	3.4%
$BR(B^0 \to K\pi)$	$(19.4 \pm 0.6) \times 10^{-6}$	3.1%	3.1%
$f_{B_d^0}/f_{B_s^0}$	3.86 ± 0.59	15.3%	-
$\epsilon^{Rel}_{B_s^0 \to e^+e^-}$	0.1290 ± 0.011	8.9%	-
$\epsilon^{Rel}_{B_d^0 \to e^+e^-}$	0.1278 ± 0.011	-	8.9%
Total		18.3%	10.0%

TABLE II: *Systematic uncertainties on the limits of* $Br(B_{s,d}^0 \to e^+e^-)$*.*

where $R = \frac{m_{B_s}}{m_b}\left(\frac{\alpha_s(M_{LQ})}{\alpha_s(m_t)}\right)^{-\frac{4}{7}}\left(\frac{\alpha_s(m_t)}{\alpha_s(m_b)}\right)^{-\frac{12}{23}}$

The values of quantities that we used in the theoretical calculation of M_{LQ} and the uncertainties thereof are listed in Table III. The strong coupling constant α_s as a function of q^2 is obtained using the Marciano approximation [20] with input value $\alpha_s(M_Z^0) = 0.115$ at the Z^0 mass pole assuming no colored particles lie between m_t and M_{LQ}.

Figure 6 shows the branching ratios $\mathrm{Br}(B_{s,d}^0 \to e^+\mu^-)$ as a function of the leptoquark mass. Using the limits on the decay branching ratio, we derive limits on the masses of the corresponding Pati-Salam leptoquarks of $\mathrm{M_{LQ}}(B_s^0) > 47.7$ (44.6) TeV/c^2 and $\mathrm{M_{LQ}}(B_d^0) > 58.6$ (55.7) TeV/c^2 at 90 (95) % confidence level.

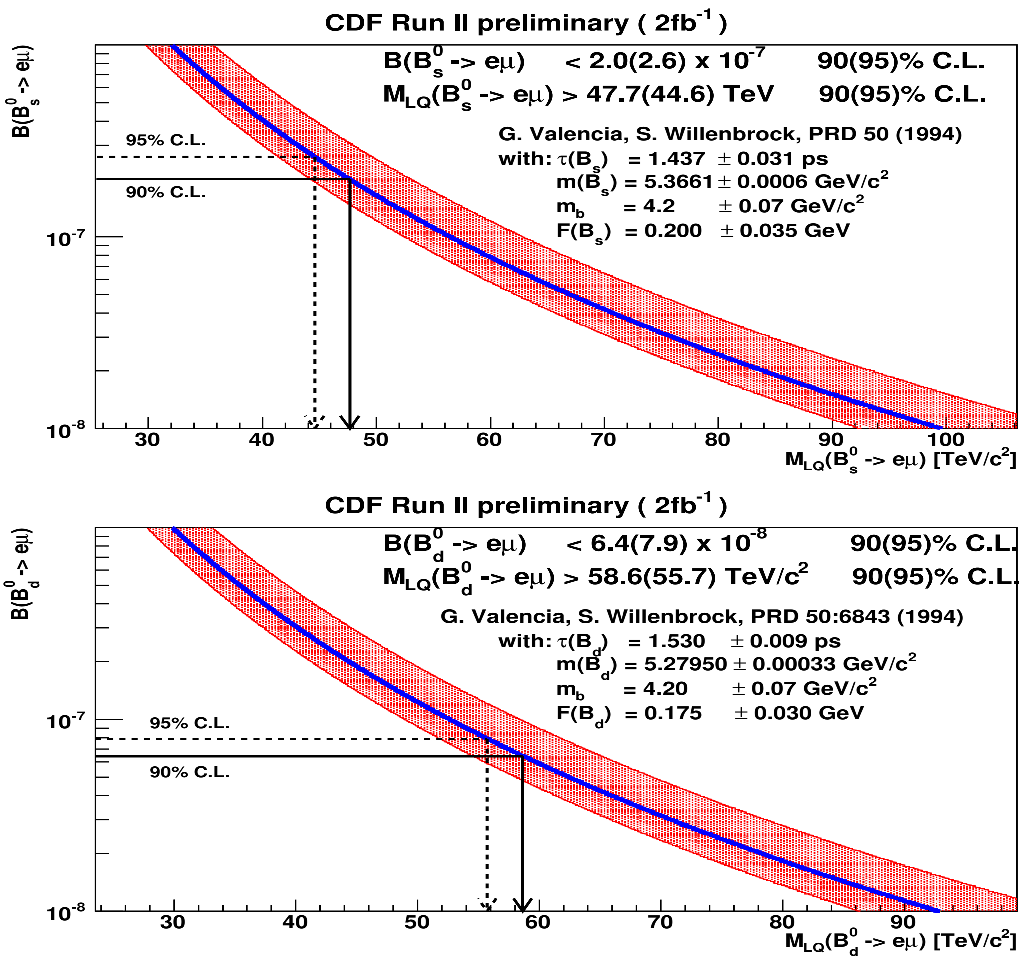

FIG. 6: Leptoquark mass limit corresponding to the 90 % C.L. on $\mathrm{Br}(B_s^0 \to e^+\mu^-)$ (top) and $\mathrm{Br}(B_d^0 \to e^+\mu^-)$ (bottom).

TABLE III: *Values of quantities used in the theoretical calculation of M_{LQ} and the uncertainties thereof.*

Quantity	Value
top quark mass: m_t	172.5 ± 2.7 GeV [17]
b quark mass: m_b	4.2 ± 0.07 GeV [17]
c quark mass: m_c	1.25 ± 0.009 GeV [17]
coupling strength: F_{B_d}	0.175 ± 0.030 GeV
coupling strength: F_{B_s}	0.200 ± 0.035 GeV
B_d-meson mass: m_{B_d}	5.27950 ± 0.00033 GeV [17]
B_s-meson mass: m_{B_s}	5.3661 ± 0.0006 GeV [17]
B_d-meson lifetime: τ_{B_d}	1.530 ± 0.009 $\times 10^{-12}$ s [17]
B_s-meson lifetime: τ_{B_s}	1.437 ± 0.031 $\times 10^{-12}$ s [17]

V. SUMMARY

Using 2 fb^{-1} of CDF Run-II data, we perform a direct searches for the lepton-flavor violating decays $B^0_{s,d} \to e^+\mu^-$ and also for the flavor changing neutral current decays $B^0_{s,d} \to e^+e^-$. No signal is observed for any of these decays. However, with 6387 ± 214 events of $B^0_d \to K^+\pi^-$ as reference channel, new upper limits on the decay branching ratios of these decays are set. For the lepton-flavor violating decays, the corresponding lower bounds on the Pati-Salam leptoquark mass are also obtained. These new results represent a significant improvement compared to CDF's previous measurement [21] and the B-Factories [22][23] [24], as shown in Table IV.

Channel	CDF Run II preliminary ($2fb^{-1}$) (@ 90(95)% C.L.)	CDF Run I ($102pb^{-1}$) (@ 90(95)% C.L.)	BARBAR (@ 90% C.L.)
$Br(B^0_s \to e^+\mu^-)$	$< 2.0(2.6) \times 10^{-7}$	$< 6.1(8.2) \times 10^{-6}$	-
$\mathrm{M_{LQ}}(B^0_s)$	$> 47.7(44.6)$ TeV/c^2	$> 20.7(19.3)$ TeV/c^2	-
$Br(B^0_d \to e^+\mu^-)$	$< 6.4(7.9) \times 10^{-8}$	$< 3.5(4.5) \times 10^{-6}$	$< 9.2 \times 10^{-8}$
$\mathrm{M_{LQ}}(B^0_d)$	$> 58.6(55.7)$ TeV/c^2	$> 21.7(20.4)$ TeV/c^2	> 53.1 TeV/c^2
$Br(B^0_s \to e^+e^-)$	$< 2.8(3.7) \times 10^{-7}$	-	-
$Br(B^0_d \to e^+e^-)$	$< 8.3(10.6) \times 10^{-8}$	-	$< 1.13 \times 10^{-7}$

TABLE IV: *Summary of results presented in this note and comparison with previous CDF results and current best limits.*

Acknowledgments

We thank the Fermilab staff and the technical staffs of the participating institutions for their vital contributions. This work was supported by the U.S. Department of Energy and National Science Foundation; the Italian Istituto Nazionale di Fisica Nucleare; the Ministry of Education, Culture, Sports, Science and Technology of Japan; the Natural Sciences and Engineering Research Council of Canada; the National Science Council of the Republic of China; the Swiss National Science Foundation; the A.P. Sloan Foundation; the Bundesministerium fuer Bildung und Forschung, Germany; the Korean Science and Engineering Foundation and the Korean Research Foundation; the Particle Physics and Astronomy Research Council and the Royal Society, UK; the Russian Foundation for Basic Research; the Comision Interministerial de Ciencia y Tecnologia, Spain; and in part by the European Community's Human Potential Programme under contract HPRN-CT-20002, Probe for New Physics.

[1] J. Pati and A. Salam, Phys. Rev. D **10** 275 (1974).
[2] R.A. Diaz, Eur. Phys. J. C **41**, 305 (2005).

A.Ilakova, Phys. Rev. D **62**,036010 (2000).
[3] G. Valencia and S. Willenbrock, Phys. Rev. D **50**, 6843 (1994).

[4] M. Blanke *et al.*, JHEP **0705**, 013 (2007)

[5] M. Misiak and J. Urban, Phys. Lett. **B 451**, 161 (1999); G. Buchalla and A. J. Burn, Nucl. Phys. **B 548**, 309 (1999).

[6] D. Acosta *et al.*, CDF Collaboration, Phys. Rev. D **71**, 032001 (2005); and references therein. 0

[7] A. Sill, *et al.*, Nucl. Instum. Methods **A 447**, 1 (2000).

[8] T. Affolder, *et al.*, Nucl. Instum. Methods **A 526**, 249 (2004).

[9] L. Balka, *et al.*, Nucl. Instum. Methods **A 267**, 272 (1988).

[10] S.Bertolucci , Nucl. Instum. Methods **A 267**, 301 (1988).

[11] G. Ascoli *et al.*, Nucl. Inst. Meth. A **268**, 33 (1988).

[12] E.J. Thomson *et al.*, IEEE Trans. Nucl. Sci. **49**, 1063 (2002).

[13] W.Ashmanskas *et al.*, Nucl. Instum. Methods **A 518**, 532 (2004).

[14] E. J. Thomson *et al.*, IEEE Trans. Nucl. Sci. **49**, 1063 (2002); A. Abulencia *et al.*, CDF Collaboration, Phys. Rev. Lett. **96**, 102002 (2006).

[15] A. Abulencia *et al.*, CDF Collaboration, Phys. Rev. Lett. **97**, 211802 (2006).

[16] A. Abulencia *et al.*, CDF Collaboration, Phys. Rev. Lett. **97**, 012002 (2006).

[17] The Particle Data Group, W.-M. Yao et al., J. Phys. G 33, 1 (2006) and 2007 partial update for the 2008 edition.

[18] Heavy Flavor Averaging Group: www.slac.stanford.edu/xorg/hfag/
ep-ex 0704.3575v1

[19] S. Eidelman *et al.*, Phys. Lett. **B 592**, 1 (2004).

[20] W. Marciano, Phys. Rev. D **29**, 580 (1984).

[21] T.Bergfeld *et al.*, CDF Collaboration, Phys. Rev. Lett. **81**, 5742 (1998).

[22] B. Aubert *et al.*, BARBAR Collaboration, Phys. Rev. Lett. **99**, 251803 (2007).

[23] M. Chang *et al.*, BELLE Collaboration, Phys. Rev. D **68**, 111101 (R) (2003).

[24] T.Bergfeld *et al.*, CLEO Collaboration, Phys. Rev. D **62**, 091102 (R) (2000).